

## EFFECT OF TIME-DEPENDENT BOUNDARY CONDITIONS ON EPIDERMAL TISSUE DAMAGE DURING PORT WINE STAIN LASER SURGERY

Guillermo Aguilar (1,2), Sergio H. Diaz Valdes (1), J. Stuart Nelson (1,2),  
and Enrique J. Lavernia (2,3)

(1) Beckman Laser Institute and Medical Clinic  
University of California, Irvine CA, 92697

(2) Center for Biomedical Engineering  
University of California, Irvine CA 92612

(3) Department of Chemical and Biochemical  
Engineering and Material Science  
University of California, Irvine CA 92612

### ABSTRACT

Port wine stain (PWS) birthmarks are a congenital and progressive vascular malformation of the dermis, involving capillaries, which occurs in approximately 0.7% of children. The objective of laser surgery for this and similar conditions is to cause selective thermal damage, thrombosis, and, eventually, permanent photocoagulation in the PWS vessels. To achieve this, the radiated laser light is set at a specific wavelength, which is highly absorbed by the blood vessels' hemoglobin (the major chromophore in blood). Unfortunately, the PWS vessels do not absorb all energy radiated—a significant amount is also absorbed by hemoglobin in the ectatic capillaries of the upper dermis. This unwanted absorption causes two problems: firstly, insufficient heat generation within the targeted vessels leads to poor clinical results, and, secondly, there is an increased risk of damage to the overlying epidermis.

In current PWS laser therapy, cryogen spray cooling (CSC) is used effectively to cool and protect selectively the epidermis (tens of micrometers thick) prior to the laser pulse, while minimally cooling the blood vessels. The thermal response of the system is characterized by time and/or temperature dependent boundary conditions. However, in many recent studies, the boundary conditions induced by CSC are regarded as constant. In the present work we study the effects of time-dependent boundary conditions on the overall epidermal thermal damage after PWS laser therapy. We use computer models to simulate the laser light distribution, heat diffusion, and tissue damage, and introduce experimentally determined time-dependent boundary conditions measured for custom-made and commercial atomizing nozzles. We show that time-dependent boundary conditions have a significant effect in the optimal laser dose required to induce photocoagulation of PWS blood vessels while preserving the epidermis.

### INTRODUCTION

Photothermal laser heating is a very useful tool in modern biomedical applications because of its accurate control on energy deposition and heat generation within diverse human tissues.

Unfortunately, in selective photothermolysis applications like the laser treatment of port wine stain (PWS) birthmarks, the absorption of light by the most superficial chromophore (epidermal melanin), not only reduces the amount of energy that can be delivered to and absorbed by the targeted chromophore (hemoglobin in the PWS blood vessels), but it also causes heating of the epidermis, which, if not controlled, may lead to blistering, scarring, or dyspigmentation [1]. The latter poses an upper limit on the maximum permissible laser radiant exposure—a major limitation for the treatment of patients with darker skin types.

Cryogen spray cooling (CSC) has been used to cool and protect selectively the epidermis (tens of micrometers thick) prior to the laser pulse, while minimally cooling the blood vessels [2]. By doing this, the laser fluence (energy per unit area) can be increased while the epidermis is protected from excessive thermal damage. Unfortunately, the current approach to CSC does not provide sufficient epidermal protection for patients with darker skin types and, consequently, light dosages are still limited to avoid non-specific thermal injury.

Recent studies have shown that current CSC may be optimized through the adjustment of parameters like nozzle diameter [3,4], nozzle-to-skin distance [5], and also by depositing the cryogen through sequential spurts [6]. Although these studies have led to important advancements in the current approach to CSC, it is clear that it is the combined effect of CSC and laser doses that determine the overall epidermal and PWS thermal damage. To appropriately select CSC parameters and laser dose, it would be desirable to perform pre-operational *in situ* tissue damage assessments. We are currently working on the development of a sub-therapeutic pulsed photothermal radiometry (PPTR) technology that will help resolve this issue. In the meantime, however, the use of heat diffusion and thermal damage models is a simpler approach, which can give an estimate of the appropriate CSC parameters and laser doses. We have simulated the combined effect of CSC and laser pulses employing numerical models of light absorption and heat diffusion, which also incorporate a thermal damage assessment in the form of an Arrhenius kinetic model. Using these models, a significant improvement in PWS laser therapy has been proposed through the use of multiple and intermittent CSC spurts

and laser pulses [7]. In all these studies, however, the boundary conditions introduced by CSC and successive laser heating are assumed constant, which is clearly a first order simplification since the thermal response of skin to CSC and laser is fundamentally a transient phenomenon, which is characterized by time and/or temperature dependent boundary conditions.

In the present work we show that using constant boundary conditions may lead to a sub-estimation of epidermal thermal damage ( $\Omega_E$ ) and, therefore, consideration of more realistic time or temperature-dependent boundary conditions is critical for the precise quantification of  $\Omega_E$ .

## MATERIALS AND METHODS

### Photothermal heating

Photothermal heating during the laser pulse is introduced as a source term ( $q$ ) into the well-known heat diffusion equation (Eq. 1):

$$\frac{1}{\alpha} \frac{\partial T}{\partial t} = \nabla^2 T + \frac{q}{k}. \quad (1)$$

The magnitude of  $q$  is computed using MCML, a Monte Carlo software package developed by Wang *et. al.* [8]. Given the specific optical properties and geometry of tissue and the shape and energy of the laser beam, MCML determines the distribution of energy deposition.

A skin model with PWS birthmark is simulated using a multi-layer geometry, consisting of four layers: an epidermal melanin layer, a normal dermis layer, a PWS layer, and another normal dermis layer with the same optical and thermal properties as the second layer (Fig. 1). For consistency, the skin layer depths and optical properties, as well as the thermal properties used in this study are the same as those used in previous studies [7,9] and are listed in Table 1. The absorption coefficient ( $\mu_a$ ) of the epidermal layer is set to  $20 \text{ cm}^{-1}$ , to describe a skin type II-III according to the Fitzpatrick classification. This absorption coefficient corresponds to melanin volume fraction ( $v_f$ ) of 5%, assuming a melanin absorption coefficient of  $400 \text{ cm}^{-1}$  at 585 nm wavelength [10]. For the normal dermis and blood energy absorption coefficients we use 2.4 and  $19.1 \text{ cm}^{-1}$ , respectively. Scattering coefficients ( $\mu_s$ ), scattering anisotropies ( $g$ ), and indices of refraction ( $n$ ) used for all layers are also listed in Table 1. The adjunct program to MCML, CONV, was used to take the infinitesimally narrow photon beam from the MCML simulations and create a flat top, circular beam with 5 mm diameter.

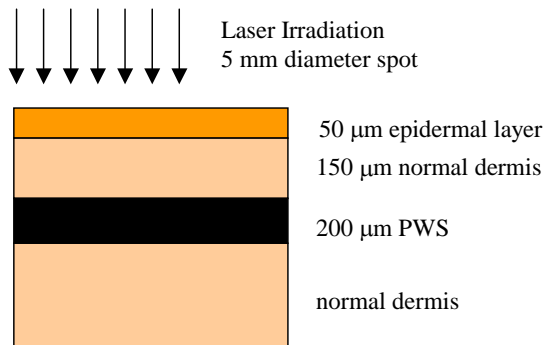


**Figure 1:** The four layer model used in the numerical simulation.

### Heat Diffusion

A forward-time centered-space (FTCS) 2D finite-difference (FD) approximation to the heat equation in cylindrical coordinates is used to compute the temperature distribution within a discrete skin model. The cross section area of the skin model is 15 mm wide and 1mm thick, and is discretized into 61 nodes spaced  $250 \mu\text{m}$  in the radial direction and 101 nodes spaced  $10 \mu\text{m}$  in the axial direction. The grid spacing for the FD heat diffusion model is the same as that of the light absorption Monte Carlo simulation. Time steps of  $100 \mu\text{s}$  ensure stability and convergence criteria.

### Boundary Conditions

Two different sets of boundary conditions are imposed to simulate the entire CSC-laser treatment, namely, those prevailing during the CSC spurt and those during and after laser irradiation. The boundary conditions during CSC are a combination of convective and evaporative cooling. They are further divided into two cases: (A) *constant* and (B) *time-dependent*. When considered *constant*, they are represented by an average spray temperature ( $T_c$ ) and an average heat transfer coefficient ( $h$ ), as in previous works [2,3,5,9]. In the *time-dependent* case, they are assumed to vary linearly as a function of time, as described in the following Section.

The boundary conditions governing during and after the energy deposition depend on the prevailing cooling medium temperature (e.g., evaporating cryogen, ice, or air), and an appropriate value of  $h$  to represent the thermal resistance of such a medium. In the present work we assumed an average  $T_c$  of  $0^\circ\text{C}$  after the laser pulse, and a constant  $h$  value of  $1,000 \text{ W/m}^2\text{K}$ .

### Experimental determination of boundary conditions

To generate the cryogen sprays, a total of three nozzles were used for this study: two custom made nozzles (referred to as *narrow nozzle*, N, and *wide nozzle*, W) of 0.7 and 1.4 mm I.D, respectively; and a commercial cryogen spray nozzle (GentleLASE™ (GL), Candela, Wayland, MA), with approximate inner diameter of 0.5 mm. Liquid cryogen (tetrafluoroethane, R-134a, boiling temperature,  $T_b = -26^\circ\text{C}$ , at atmospheric pressure) was delivered through a standard high-pressure hose connecting the container to a control valve. The container is pressurized at the saturation pressure of this cryogen (6.7 bar at  $25^\circ\text{C}$ ). Spurt durations—defined by the time the valve remains open, were fixed at 100 ms and electronically controlled.

To estimate  $T_c$  during CSC, a type-K thermocouple with bead diameter of approximately 0.3 mm (5SC-TT-E-36 by Omega, Stamford, CT) was supported by a rigid stick and inserted into the center of the spray cone at 50 mm from the nozzle. A custom-made device was built to measure the heat transfer coefficient ( $h$ ). In short, the device consists of a silver disk (10.48 mm diameter, 0.42 mm thickness), embedded in a thermal insulator, e.g., epoxy. Further details about the construction and measurement procedure using this device may be found elsewhere [5,9].

### Tissue Damage ( $\Omega$ )

Tissue thermal damage was computed using the Arrhenius-type kinetic model, given by Eq. 2, as follows:

$$\Omega(t) = \int_0^t A \exp(-E_a / RT) dt \quad (2)$$

where  $A$  is a frequency factor [1/s],  $E_a$  an activation energy barrier [J/mole],  $R$  the universal gas constant [8.32 J/mole K], and  $T$  the absolute temperature [K]. The computations of  $\Omega$  were incorporated into the finite-difference heat diffusivity model and calculated for each

time step starting at the beginning of the laser pulse. The parameters  $A$  and  $E_a$  used in this study are listed in Table 2, and also correspond to the values used in previous studies [7,9,11].

The epidermal damage ( $\Omega_E$ ) was computed 50  $\mu\text{m}$  below the skin surface, which is the average depth of the epidermal basal layer—the site where maximum protection is needed. Excessive damage was considered to have occurred when values for  $\Omega_E$  were higher than 1, which corresponds to a 63% decrease from the original total of undamaged tissue constituents. If this critical value was reached, the computation stopped and the program warned that excessive tissue damage had occurred. Computations are carried out for an absolute time ( $t$ ) of 600 ms. Beyond this time, it is considered that  $\Omega_E$  changes insignificantly.

## RESULTS AND DISCUSSION

Figure 2 shows experimental measurements of  $T_c(t)$ ,  $h(t)$ , and  $q(t)$  for the N,W, and GL nozzles. All plots are smoothed curves representing the average of five measurements. As noted, the W nozzle shows the lowest  $T_c$  during most of the spurt duration, and the highest and steadier value of  $h(t)$  and  $q(t)$ . In contrast, the N and GL nozzles (0.7 and 0.5 mm I.D., respectively) show higher values of  $T_c(t)$  up to  $t = 68$  ms, and large fluctuation in  $h(t)$  and  $q(t)$ , especially during the first 40 ms.

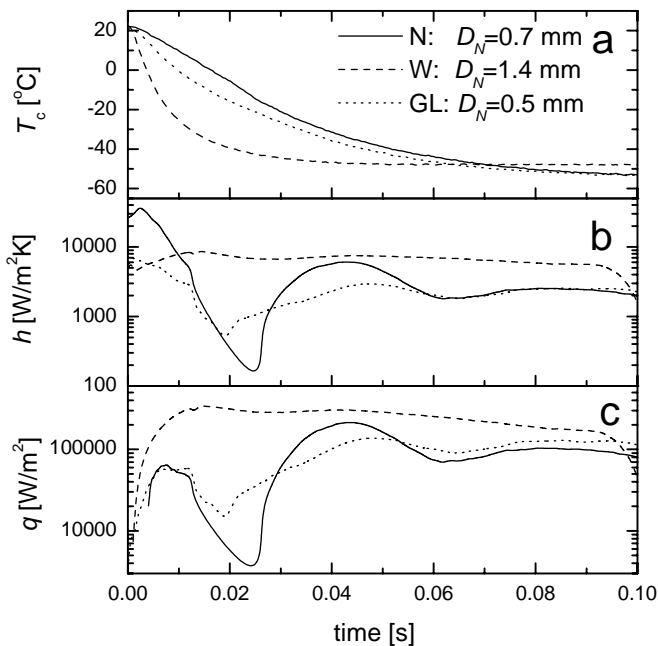


**Fig. 2.** Spray temperature ( $T_c$ ), heat transfer coefficient ( $h$ ), and heat flux through the surface ( $q$ ) as a function of time for 100 ms spurts produced by three nozzles: N, W, and GL. Each curve represents an average of five identical measurements and the resulting curves for  $h$  and  $q$  have been smoothed using a FFT algorithm.

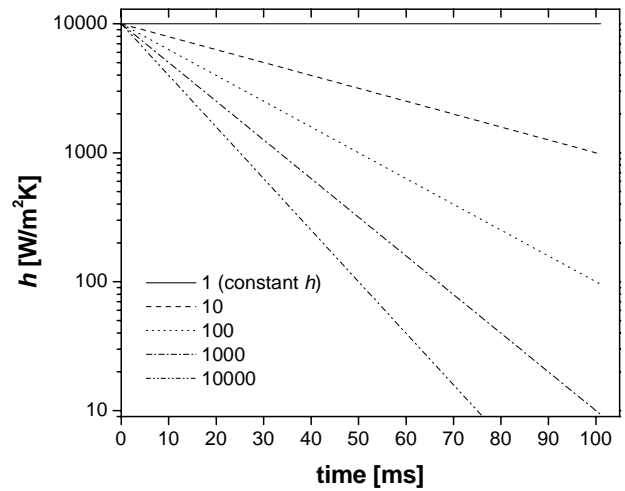
In order to study the effect of the CSC boundary conditions, i.e.,  $h(t)$  and  $T_c(t)$  on the overall epidermal thermal damage ( $\Omega_E$ ), we used the FD code to predict the skin temperature after a 100 ms spurt was simulated for two different cases of boundary conditions : (A) *Constant* and, (B) *Time-dependent*  $h$  and  $T_c$ .

(A) *Constant*  $h$  and  $T_c$ : The values of  $h$  and  $T_c$  were fixed at 10,000  $\text{W}/\text{m}^2$  K and  $-60^{\circ}\text{C}$ , respectively. These values represent an ideal, but yet achievable situation, with a sufficiently large value of  $h$  and

minimal  $T_c$  to maximize the heat extraction [6]. No delay between the end of the spurt and the beginning of the laser pulse was allowed, as suggested by Verkruysse et al. [2].

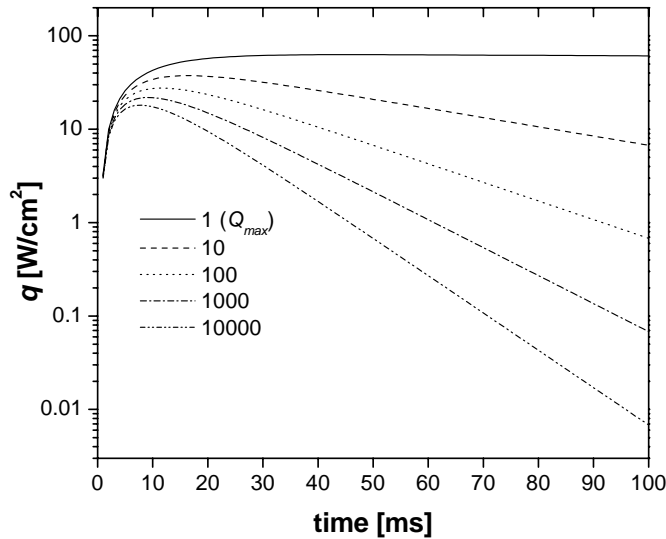
(B) *Time-dependent*  $h(t)$  and  $T_c(t)$ : These values were determined based on the experimental procedures (Fig. 2a,b). However, we introduced into the FD model a linear decrease of  $h(t)$  in a semi-log scale, as a simplification to account for the experimentally observed variations.

Figure 3 shows a series of lines corresponding to a different decrease rate factor of  $h(t)$ . As a reference, a factor of 100 represents in these coordinates a decrease in  $h$  of two orders of magnitude during the 100 ms spurt, which is the order of magnitude of the variation of  $h(t)$  for the N nozzle during the first 25 ms (Fig.2b). The corresponding heat flux,  $q(t)$ , for each curve of  $h(t)$ , is shown in Fig.4. This parameter is computed as  $q(t) = h(t) (T_s(t) - T_c(t))$ , where  $T_s(t)$  is the instantaneous surface temperature as resulting from the exact solution of the 1-D heat conduction equation (Eq. 1) in a semi-infinite solid, subject to a convective boundary condition, and  $T_c(t)$  is the cryogen temperature corresponding to the W nozzle, as shown in Fig.2a.



**Fig. 3** Heat transfer coefficient as a function of time. Each curve represents an arbitrary variation of  $h$  with time, starting from a maximum value of 10,000  $\text{W}/\text{m}^2\text{K}$  and decaying linearly in semi-log coordinates according to the factor specified within the Figure.

Evidently, the ideal situation of a constant  $h = 10,000$   $\text{W}/\text{m}^2\text{K}$  and constant  $T_c = -60^{\circ}\text{C}$  (case A) would lead to a maximal heat extraction. The total amount of heat per unit area removed from the silver disk under such conditions ( $Q_{max}$ ) is equal to 5.76  $\text{J}/\text{cm}^2$ . Therefore, the corresponding  $Q$  for each decrease rate factor may be computed by integrating each of the curves shown in Fig.4 and normalized by  $Q_{max}$  leading to the curve shown in Fig. 5. As a reference, the measured  $Q$  values corresponding to the N, W, and GL nozzles, are represented by the markers in the same Figure. In either case (A and B), the boundary conditions during and after laser exposure were fixed at:  $h = 1,000$   $\text{W}/\text{m}^2\text{K}$  and  $T_c = 0^{\circ}\text{C}$ . This boundary condition presumably simulates the presence of a thin layer of frozen water, which slowly evaporates over time.



**Fig. 4** Heat flux at the sprayed surface ( $q$ ) as a function of time.  $q(t)$  is computed by multiplying the corresponding  $h$  curves illustrated in Fig. 3, by the surface to spray temperature difference, i.e.,  $T_s(t) - T_c(t)$ .  $T_s(t)$  is the instantaneous surface temperature as resulting from the exact solution of the 1-D heat conduction equation in a semi-infinite solid, subject to a convective boundary condition, and  $T_c(t)$  is the cryogen temperature corresponding to the W nozzle, as shown in Fig.2a.

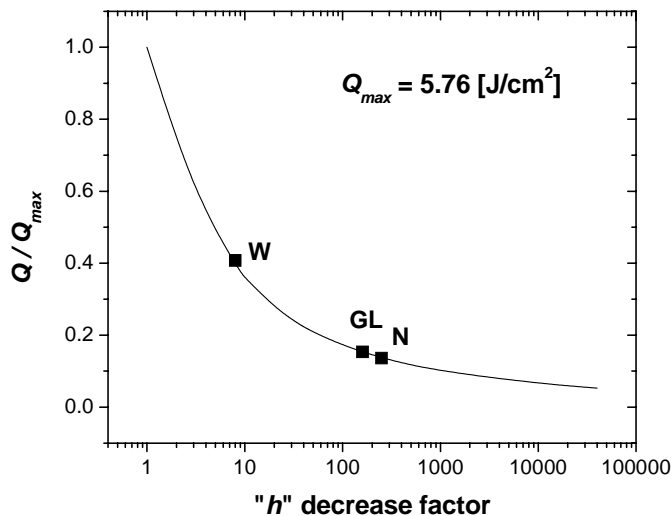


**Fig. 5.** Total amount of heat ( $Q$ ) removed by a 100 ms cryogen spurt as a function of the decrease rate factor of  $h$ .  $Q$  is normalized by  $Q_{max}$ , which is the maximum amount of heat that can be removed by a cryogen spurt with a constant boundary condition having values of:  $h = 10,000 \text{ W/m}^2\text{K}$  and  $T_c = -60^\circ\text{C}$ . The markers illustrate the experimentally determined  $Q$  for the three nozzles of study: N,W, and GL.

Figure 6 shows an example of  $\Omega_E$  as a function of  $Q/Q_{max}$ . A 1.5 ms laser pulse of  $10 \text{ J/cm}^2$  is applied to a skin type II-III (corresponding to a  $v_f = 5\%$ ) and  $h(t)$  is allowed to vary according to different decrease rate factors. In all cases, the laser pulse is triggered

immediately after the 100 ms cryogen spurt and the iterations continue up to a total time of 600 ms. This example shows a case where assuming a constant boundary condition with an  $h$  value of  $\sim 10,000 \text{ W/m}^2\text{K}$  may indicate that epidermal protection is sufficient. However, for decrease rate factor of  $\sim 40$ , corresponding to  $Q/Q_{max} < 0.22$  (as the N and GL nozzles provide), severe epidermal damage may be attained. Note that the W nozzle, however, would provide much lesser damage ( $\Omega_E < 0.01$ ).

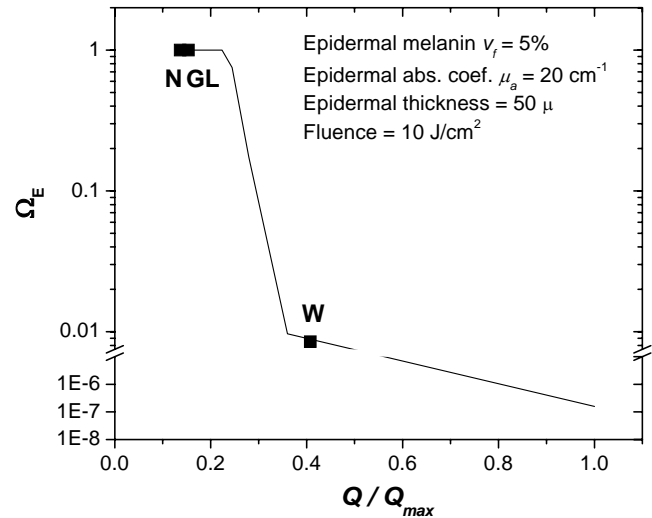


**Fig. 6.** Epidermal damage ( $\Omega_E$ ) as a function of the total amount of heat ( $Q$ ) removed by a 100 ms cryogen spurt. This example assumes a  $10 \text{ J/cm}^2$  applied to a skin type II-III (corresponding to  $v_f = 5\%$ ) and a  $50\mu\text{m}$  thick epidermis. Values of  $Q/Q_{max} < 1$  correspond to decrease rate factors of  $h$  as illustrated in Fig. 5. The markers illustrate the computed epidermal damage ( $\Omega_E$ ) based on the experimentally determined  $Q$  for the three nozzles of study: N,W, and GL.

Another representation of the same idea is shown in Fig. 7 for the same example ( $v_f = 5\%$ ). In this case, the maximal permissible fluence, i.e., the fluence which leads to  $\Omega_E = 1$ , is plotted as a function of  $Q/Q_{max}$ . As noted, a patient with  $v_f = 5\%$  may be safely treated with a fluence of  $13 \text{ J/cm}^2$  provided CSC provides a boundary constant with an ideal constant magnitude of  $h = 10,000 \text{ W/m}^2\text{K}$  (i.e.,  $Q = Q_{max}$ )—close to what the W nozzle could provide. However, for lower values of  $Q/Q_{max}$ , the laser dose should definitely be reduced to protect the epidermis. Considering the variations seen for the N and GL nozzles, a reduction of 30% from the maximal ideal fluence would be desirable.

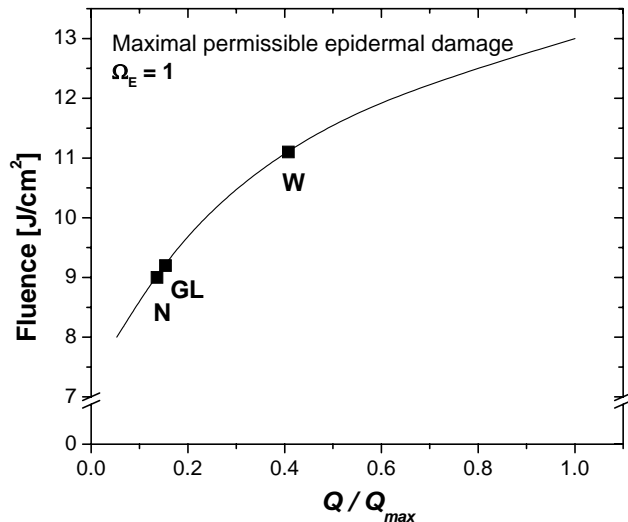


**Fig. 7.** Maximal permissible fluence, i.e., fluence which leads to  $\Omega_E = 1$ , plotted as a function of  $Q/Q_{max}$  for the same example illustrated in Fig.6. The markers illustrate the maximal fluence suggested for the three nozzles of study: N,W, and GL based on the experimentally determined  $Q$  for each of them.

## CONCLUSIONS

We have shown that the inclusion of time-dependent boundary conditions, as experimentally determined from custom-made and commercial atomizing nozzles, is critical in the precise quantification of epidermal thermal damage ( $\Omega_E$ ) during PWS laser therapy. This damage parameter, in turn, is critical for the selection of the maximum laser dose required to induce blood coagulation while preserving the epidermis.

## ACKNOWLEDGEMENTS

This work was supported by a research grant from the Institute of Arthritis and Musculoskeletal and Skin Diseases at the National Institutes of Health (AR43419 to JSN). Institutional support from the Office of Naval Research, Department of Energy, National Institutes of Health, and the Beckman Laser Institute and Medical Clinic Endowment is also acknowledged.

## REFERENCES

1. Chang, C.J., and Nelson, J.S., 1999, "Cryogen spray cooling and higher fluence pulsed dye laser treatment improve port-wine stain clearance while minimizing epidermal damage," *Dermatol. Surg.*, Vol. 25, pp. 767-772.
2. Verkruysse, W., Majaron, B., Tanenbaum, B.S., and Nelson, J.S., 2000, "Optimal cryogen spray cooling parameters for pulsed laser treatment of port wine stains," *Lasers Surg. Med.*, Vol. 27, pp. 165-170.
3. Verkruysse, W., Majaron, B., Aguilar, G., Svaasand, L.O., and Nelson, J.S., 2000, "Dynamics of cryogen deposition relative to heat extraction rate during cryogen spray cooling," *Proc. SPIE*, Vol. 3907, pp. 37-58.
4. Aguilar, G., Verkruysse, W., Majaron, B., Svaasand, L.O., Lavernia, E.J., and Nelson, J.S., 2001, "Measurement of heat

flux and heat transfer coefficient during continuous cryogen spray cooling for laser dermatologic surgery". *Submitted to IEEE J Special Topics Quant Elect.*

5. Aguilar, G., Majaron, B., Pope, K., Svaasand, L.O., Lavernia, E.J., and Nelson, J.S., 2001, "Influence of nozzle-to-skin distance in cryogen spray cooling for dermatologic laser surgery," *Lasers Surg Med.*, Vol. 28, pp. 113-120.
6. Majaron, B., Aguilar, G., Basinger, B., Randeberg, L.L., Svaasand, L.O., Lavernia, E.J., and Nelson, J.S., 2001, "Sequential cryogen spraying for heat flux control at the skin surface," *Proc SPIE*, Vol. 4244, pp. 74-81.
7. Aguilar, G., Lavernia, E.J., and Nelson, J.S., 2001, "Definition and expected benefit of maximum cryogen spray cooling efficiency during port wine stain laser therapy. Improvement through multiple-intermittent cryogen spurts and laser pulses", *submitted to Lasers in Surgery and Medicine*.
8. Wang, L. and Jacques, S.L., 1992, Monte Carlo modeling of light transport in multi-layered tissues in standard C.", University of Texas M. D. Anderson Cancer Center.
9. Aguilar, G., Majaron, B., Viator, J.A., Basinger, B., Karapetian, E., Svaasand, L.O., Lavernia, E.J., and Nelson, J.S., 2001, "Influence of spraying distance and post-cooling on cryogen spray cooling for dermatologic laser surgery", *Proceedings SPIE*, San Jose CA, Jan 20-25, Vol. 4244, pp. 82-92.
10. Jacques, S.L., Glickman, R.D., and Schwartz, J.A., 1996, "Internal absorption coefficient and threshold for pulsed laser disruption of melanosomes isolated from retinal pigment epithelium," *Proc. SPIE*, Vol. 2681, pp. 468-477.
11. Pfefer, T.J., Smithies, D.J., Milner, T.E., van Gemert, M.J.C., Nelson, J.S., and Welch, A.J., 2000, "Bioheat transfer analysis of cryogen spray cooling during laser treatment of port wine stains," *Lasers Surg Med*, Vol. 26, pp. 145-157.